NANO LETTERS

Letter

pubs.acs.org/NanoLett

Adsorption and Diffusion of Lithium on Layered Silicon for Li-Ion Storage

Georgios A. Tritsaris,[†,‡] Efthimios Kaxiras,[†,§] Sheng Meng,[∥,*] and Enge Wang[‡]

[†]School of Engineering and Applied Sciences, Harvard University, Cambridge, Massachusetts 02138, United States

[‡]International Center for Quantum Materials, Peking University, No. 5 Yiheyuan Road, Haidian District, Beijing 100871, China

[§]Department of Physics, Harvard University, Cambridge, Massachusetts 02138, United States

[∥]Institute of Physics, Chinese Academy of Sciences, Beijing 100190, China

ABSTRACT: The energy density of Li-ion batteries depends critically on the specific charge capacity of the constituent electrodes. Silicene, the silicon analogue to graphene, being of atomic thickness could serve as high-capacity host of Li in Li-ion secondary batteries. In this work, we employ first-principles calculations to investigate the interaction of Li with Si in model electrodes of free-standing single-layer and double-layer silicene. More specifically, we identify strong binding sites for Li, calculate the energy barriers accompanying Li diffusion, and present our findings in the context of previous theoretical work related to Li-ion storage in other structural forms of silicon: the bulk and nanowires. The binding energy of Li is ∼2.2 eV per Li atom and shows small variation with respect to Li content and silicene thickness (one or two layers) while the barriers for Li diffusion are relatively low, typically less than 0.6 eV. We use our theoretical findings to assess the suitability of two-dimensional silicon in the form of silicene layers for Li-ion storage.

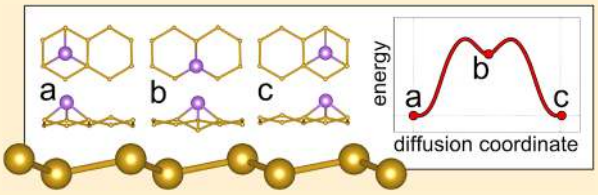

KEYWORDS: *Lithium-ion battery, energy storage, two-dimensional silicon, adatom adsorption, surface diffusion, ab initio calculations*

Li-ion secondary batteries constitute a promising energy storage technology suitable for portable and grid applications. Their energy density depends critically on the specific charge capacity of the constituent electrodes.[1,2] Si-based anodes are investigated as an alternative to the conventional graphite anode because of their high theoretical specific capacity (4200 mAh g^{-1}),[2−5] although the degradation of silicon that accompanies battery operation and the subsequent reduction in charge rate have limited the commercialization of this battery technology.[6−10] In line with the prevalent interest in two-dimensional layered materials[11−13] the preparation of single-layer and few-layer, graphene-like structures of silicon referred to as "silicene" has been recently reported.[14−16] Control of silicene synthesis is continuously improving with samples having been prepared thus far on various metal substrates, for instance, Ag, Ir, and ZrB_2.[15,17−20] There is also an ongoing effort to better understand the properties of low-dimensional silicon through theory and simulation.[17,21−30] Owing to its large surface area, silicene could serve as high-capacity host of Li in Li-ion secondary batteries. Within this broad context, the interaction of Li with single-layer and few-layer silicene remains largely unexplored.[31,32]

To assess the suitability of silicene as a host material for Li, we use first-principles calculations based on density functional theory in this work to study the local interaction of Li with Si in model, free-standing single-layer and double-layer structures of silicene. Theoretical calculations can provide atomic-level insight into the kinetics of the diffusion of Li in bulk and two-dimensional structures of silicon, which is difficult to obtain solely by experimental means.[7,10,33−35] Specifically, we identify the binding sites for Li and we calculate the energy barriers for Li diffusion. We find that the binding energy (∼2.2 eV/Li atom) shows small variation as a function of Li content and the number of Si layers (one or two), and energy barriers for Li diffusion that are typically smaller than those for diffusion in bulk silicon and thin silicon nanowires (<0.6 eV).

We modeled a free-standing single-layer structure of silicene using a two-atom unit cell with lattice constant a_{sl} = 3.88 Å, where the Si atoms are in a puckered honeycomb lattice arrangement and the bond length is 2.28 Å. The distance between two nearest neighbor Si atoms projected on the axis perpendicular to the plane is 0.44 Å. The optimized atomic configuration is in agreement with previous theoretical work.[26,36,37] We also optimized the geometry of structures that consist of two silicene layers stacked together in either AA or AB arrangement. The lowest-energy structure corresponds to the AA arrangement with lattice constant a_{dl} = 4.13 Å (the bond length within each layer is 2.39 Å), no puckering (in contrast to the case of the single-layer structure of silicene) and a distance between the atomic layers of 2.41 Å. We used this configuration to study the interaction of Li atoms with the double-layer silicene. For the calculation of adsorption energies, we used 2 × 2 supercells (Figure 1), and a void region of 15 Å

Received: March 6, 2013
Revised: April 12, 2013
Published: April 19, 2013

   dx.doi.org/10.1021/nl400830u | *Nano Lett.* 2013, 13, 2258−2263

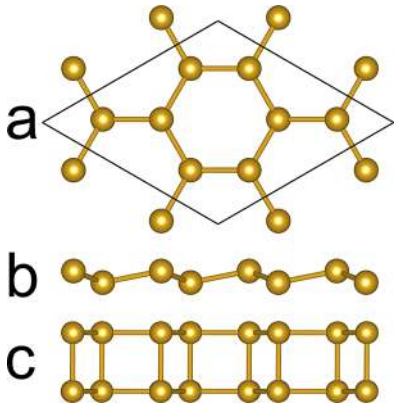

Figure 1. Structural models of silicene. (a,b) Top and side views of single-layer silicene; (a,c) top and side views of double-layer silicene.

separating the layers was included in the direction perpendicular to the silicene plane to ensure that the wave functions vanish smoothly at the edge of the cell as would be required in an isolated system. In the following, we use the notation Li_xSi_{1-x} to distinguish between different (fractional) content, x, of Li. The value of $x = 0$ corresponds to the pristine silicene layer. Silicene-type silicon in the form of nanoribbons has also been synthesized,[14] but in this work we have elected to model only extended sheets of silicene to avoid the complications of finite size effects on the energetics of adsorption and diffusion of Li.[34]

We performed total energy calculations using the GPAW code,[38] a grid-based approach based on the projected augmented-wave method.[39] For the description of exchange and correlation we used the Perdew–Burke–Ernzerhof functional.[40] We also performed calculations within the local density approximation and we found no difference in the relative stability of the calculated atomic configurations. A Monkhorst–Pack mesh of $6 \times 6 \times 1$ special points was used for integration in reciprocal space. For structural optimizations, the magnitude of forces on atoms was minimized to be below the limit of 0.04 eV/Å. To obtain diffusion pathways and the corresponding energy barriers, we performed standard nudged elastic band (NEB) calculations.[41] For each pair of configurations with Li in equivalent binding sites we sampled the corresponding pathway for diffusion with a NEB path consisting of eight intermediate configurations. The NEB path was first constructed by linear interpolation of the atomic coordinates and then relaxed until the force on each atom was smaller in magnitude than 0.04 eV/Å. A continuous diffusion path was obtained by polynomial interpolation between the optimized configurations.

The first step in investigating the diffusion pathways of Li is to identify atomic structures of lithiated silicene corresponding to equilibrium configurations for a given system composition. To this end, we calculated the binding (adsorption) energy per Li atom, E_b, using the expression $E_b = E_0 + xE_{Li} - E_x$, where E_x denotes the total energy of the lithiated structure, E_0 is the total energy of the pristine silicene layer, and E_{Li} is the energy of an isolated Li atom. In this scheme, the higher the value of E_b, the stronger the binding of Li to silicene. Hereafter, we use the terms "binding" and "adsorption" interchangeably.

We discuss first the case of adsorption on single-layer silicene (Figure 2). For a single Li adatom in the unit cell (SL-$Li_{0.11}Si_{0.89}$) the most stable adsorption site is the hollow site, where Li resides above the center of the hexagonal silicene ring and it has three nearest neighbor Si atoms. The corresponding adsorption energy is 2.08 eV (values of 2.13 and 2.21 eV for this energy have been reported in previous theoretical studies).[31,32] The coordination is calculated using a cutoff distance of 2.7 Å, which corresponds to the length of the bond between a Li atom at a "tetrahedral" site and its second nearest Si atom neighbors in bulk crystalline silicon.[10,42] We also calculate $E_b = 2.12$ eV for a single Li adatom in a (3×3) supercell ($x = 0.06$), which suggests that the interaction between the Li atoms at the coverage of $x = 0.11$ is already negligible. Adsorption directly above a Si atom or at the bridge site between two neighbor Si atoms is weaker with $E_b = 1.89$ eV and $E_b = 1.68$ eV, respectively. The hollow site remains the most stable adsorption site for Li for the structure corresponding to SL-$Li_{0.20}Si_{0.80}$ for which we obtain $E_b = 2.19$ eV. In this case, half the Li atoms are adsorbed above and half below the silicene layer. At moderate Li coverage ($x = 0.33$) stripes of Li form on each side of the silicene layer and the most stable atomic configuration shifts from adsorption at the hollow site to adsorption directly above the Si atoms with $E_b = 2.19$ eV. In the structure corresponding to SL-$Li_{0.50}Si_{0.50}$ half the Li atoms are adsorbed above and half below the silicene layer in a

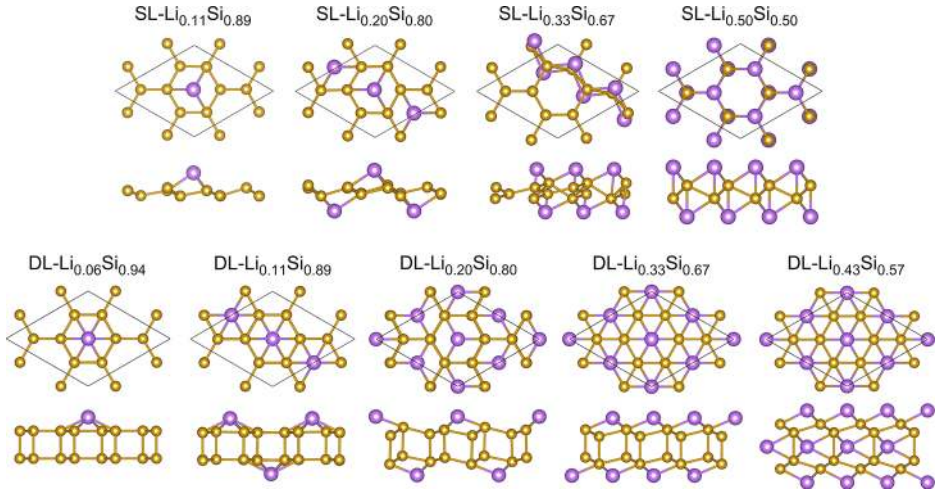

Figure 2. Atomic structures corresponding to lithiated single-layer (SL) and double-layer (DL) silicene, Li_xSi_{1-x} of varying Li content, x. The unit cell is outlined in each top view; top and side views are shown separately.

dx.doi.org/10.1021/nl400830u | *Nano Lett.* 2013, 13, 2258–2263

similar fashion as in SL-$Li_{0.33}Si_{0.67}$ and the corresponding adsorption energy is 2.28 eV. For $x > 0.50$ the binding of Li is weakened significantly. For instance, at the Li content of $x = 0.67$ where both surfaces of the silicene layer are covered by Li, with one Li adatom adsorbed above and one Li adatom adsorbed below each Si atom, the adsorption energy is 1.75 eV, which indicates increased repulsion between the Li atoms within the Li adlayers. Therefore we use SL-$Li_{0.50}Si_{0.50}$ to represent the fully lithiated configuration of single-layer silicene. We further optimized the unit cell of SL-$Li_{0.50}Si_{0.50}$ and we find the lattice constant of the optimized structure to be 3.72 Å (the length of the Si−Si bond is 2.39 Å), that is, 4% smaller than that of the pristine silicene layer. This optimization reduces the total energy by 0.10 eV (E_b = 2.38 eV).

We summarize how the adsorption energy varies with increasing Li content in Figure 3. In going from the pristine to

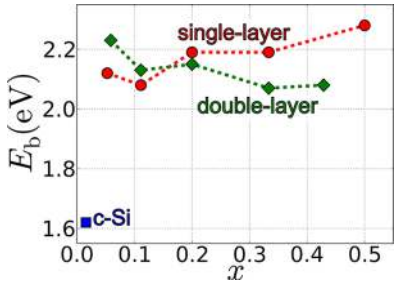

Figure 3. Binding energy, E_b, of Li as a function of Li content, x, for single-layer (red) and double-layer (green) silicene, Li_xSi_{1-x}. The blue point marks the binding energy of Li in bulk crystalline silicon (c-Si) in the low-concentration limit ($x = 1/64$).

the fully lithiated single-layer silicene the adsorption energy varies little within a range of energy that spans only 0.20 eV. The small variation is in agreement with previous theoretical results.[31] Assuming no additional energy barriers to the kinetic transport of Li in the material, the small variation in adsorption energy suggests that lithiation should be spontaneous if a potential difference of ∼2.2 V is applied.

We also modeled a highly puckered structure of single-layer silicene with lattice constant 2.68 Å and distance between the two atomic planes 2.17 Å,[27] found by energy minimization as a function of the in-plane lattice constant when the latter is in the range between 2.0 and 3.0 Å. Upon adsorption of a Li atom, this silicene layer reconstructs to accommodate the Li atom by substitution of one Si atom that is displaced out of the surface. Moreover, after removal of the Li atom from the system the structure does not return to its initial form. These findings indicate that highly puckered silicene is not thermodynamically stable during repeating lithiation and delithiation cycles; hence, we do not consider this structure further.

We discuss next a model double-layer structure of silicene (Figure 1a,c). To confirm that the double-layer structure is stable in its own right, we calculated the binding energy of the two atomic Si layers or equivalently the energy needed to separate them to infinite distance and find it to be 0.19 eV per Si atom. As an additional check of stability, we performed molecular dynamics simulations for 1.0 ps in the micro-canonical ensemble (N, V, E) at the relatively high temperature of 600 K with a time step of 1.5 fs and obtained the average bond length from configurations encountered during the last 0.5 ps with a sampling rate of 1/50 fs^{-1}. We find that even at this temperature the average deviation of bonds from their ground-state value is rather small (∼3%) that we attribute to strong Si−Si bonding.[24] These findings support the stability of free-standing double-layer silicene, although unsupported silicene has not yet been observed experimentally.

In Figure 2f,g, we show atomic structures of lithiated double-layer silicene for varying Li content. As was the case in the single-layer structure, a Li adatom adsorbs preferably above the center of the six-atom silicene ring with E_b = 2.23 eV, but in the case of double-layer silicene it is situated closer to the surface with six nearest neighbor Si atoms. Binding of Li at the hollow site between the two atomic layers is less favorable and so is binding directly above a Si atom with E_b = 1.96 eV and E_b = 1.48 eV, respectively. In contrast to the case of the single-layer structure, the hollow site remains the most favorable site for Li adsorption at higher Li content. With increasing Li adsorption, Li atoms gradually cover the two external surfaces of the double-layer silicene and in the fully lithiated structure, DL-$Li_{0.43}Si_{0.57}$, the hollow sites in the interior of silicene become occupied too (E_b = 2.08 eV). We calculate the total energy of DL-$Li_{0.43}Si_{0.57}$ to be 0.90 eV per unit cell less than the combined total energy of SL-$Li_{0.33}Si_{0.66}$ and SL-$Li_{0.50}Si_{0.50}$, which together have the same Li and Si content with the double-layer structure, an indication that double-layer silicene does not exfoliate with Li intercalation. At even higher Li content, for instance when one Li atom is adsorbed on each Si atom, the binding between Si and Li weakens significantly, resulting in E_b = 1.03 eV.

In Figure 3, we show the trend in the binding energy of Li as a function of the Li content for the model double-layer silicene, compared with the corresponding findings pertaining to the single-layer structure. Interestingly, the adsorption energies vary in the range between 2.08 and 2.23 eV, which is quite similar to that for adsorption of Li on the single-layer structure. These energies should be contrasted to the binding energy of a single Li impurity at an interstitial "tetrahedral" site (four nearest neighbor Si atoms) in bulk crystalline silicon which is 1.62 eV,[10,42] that is, Li binds stronger to silicene than in bulk crystalline silicon. Binding to silicene is also stronger in comparison to the case of thin silicon nanowires for which calculated binding energies are typically less than 1.6 eV.[29,34] According to Figure 3, the working potential of an electrode based on free-standing silicene should be relatively flat, which happens to be one of the attractive features of graphite, the most commercially successful anode material. Theory also predicts the specific charge capacity of silicene to be 954 and 715 mAh/g for the single-layer and double-layer respectively, which is significantly higher than this of graphite, 372 mAh/g. We note that in some cases the energy difference between two calculated atomic configurations is of the order of DFT error. For example, for SL-$Li_{0.20}Si_{0.80}$ a configuration where two Li atoms are adsorbed above and below the same hollow site is only 0.04 eV higher in energy than the most stable configuration. The reported adsorption energies are not corrected with zero-point energy and entropic contributions. Such corrections could change the relative stability of atomic configurations that lie close in total energy, but we do not expect the general trends in adsorption presented in Figure 3 to be affected.

In general, with increasing Li content the silicene layer shows progressively the signature of an sp^3-bonded atomic arrangement: the distortion of the surface is pronounced in SL-$Li_{0.50}Si_{0.50}$ where the distance between the atomic planes is 1.05 Å,[31] and the initially flat atomic layers in pristine double-layer silicene become puckered in DL-$Li_{0.43}Si_{0.57}$ where the distance

dx.doi.org/10.1021/nl400830u | Nano Lett. 2013, 13, 2258−2263

between the top (bottom) two atomic planes is 0.74 Å and the central Si atoms have bond angles of 107°. To associate an effective volume with these layered structures, we define the thickness of silicene as the distance between the two external atomic planes augmented by twice the van der Waals radius of Si, 2.1 Å. We can then conclude that upon lithiation the overall change in the volume of the silicene layer is small, 13% and 24% for the single-layer and double-layer structures, respectively. This should be compared to the almost 4-fold volumetric expansion of bulk crystalline silicon upon full lithiation.[5] After complete delithiation, the silicene surface is restored to the form of the pristine structure in contrast to crystalline silicon which undergoes severe structural changes due to plastic deformation.[5,42,43]

We explain the trend in adsorption energies of Figure 3 as follows. Li, as other alkali and alkali-earth metal adatoms, bound to silicene acts as an n-type dopant.[32] Using Bader analysis[44] we find that each Li atom donates a charge of ∼0.8 *e* to the silicene layer to saturate the Si bonds. This is more evident at low Li coverage where Li adsorbs at high-coordination sites (see also Figure 2). At high Li coverage, the electronic effect is manifested geometrically with the expansion of the Si−Si bonds in the direction perpendicular to the surface. For nonoptimal adsorption, we find that the same amount of charge is transferred from Li to silicene but the position of the Li atoms do not allow the silicene surface to reconstruct and reduce the induced strain in the Si−Si bonds. Adsorption of Li on silicene can be understood as a two-step process, shown schematically in Figure 4 for the single-layer structure. First, electrons are transferred from Li to the valence band of silicene, which is rendered metallic (the band gap of the free-standing single-layer silicene is zero). The silicene surface then relaxes in an effort to saturate the bonds and relieve the strain within the Si rings. In doing so, the band gap reopens: upon full lithiation the band gap of the initially pristine silicene layer widens from zero to 0.32 eV (a value of 0.37 eV has been reported in previous theoretical work),[31] roughly half the value calculated for the band gap of bulk crystalline silicon (0.59 eV). The cooperative effect between static charge transfer and strain relief in the silicene layer thus maintains almost constant adsorption energy values upon adsorption of Li in varying content.

We next shift our attention to the motion of a Li atom on silicene. We used the NEB method to study the diffusion of a single Li adatom on single-layer silicene by calculating the variation in energy as Li moves between equivalent adsorption sites. The diffusion coordinate is the cumulative sum of the trajectory length of all atoms in the structure since the diffusion process involves cooperative motion of several atoms simultaneously, including the Li adatom and its Si neighbors. In Figure 5a–k, we show examples of elementary hops of Li on the single-layer silicene. An important consideration for studying the diffusion of Li is the Li content. In the low-

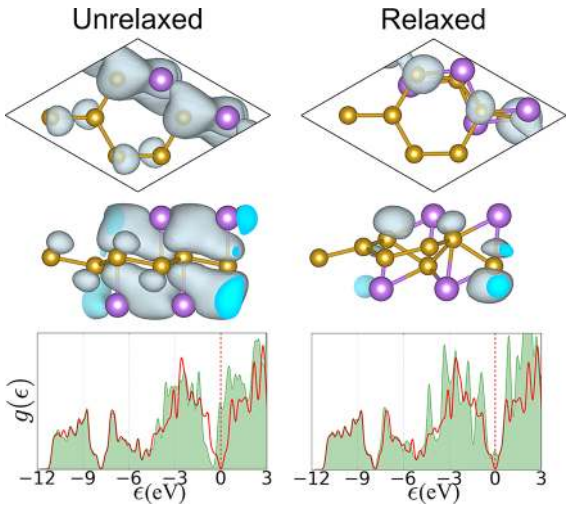

Figure 4. Isosurfaces corresponding to the wave function associated with the occupied state at the center of the Brillouin zone closest to the Fermi level for the single-layer silicene with moderate Li coverage: (a) before and (b) after relaxation of the Si atoms (top and side view are shown separately). The density of states, $g(\varepsilon)$, (green shaded curve) in each case is compared with the density of states of the pristine silicene layer (red solid line). The vertical dashed line marks the middle of the band gap of the pristine structure, defined as the zero of the energy scale.

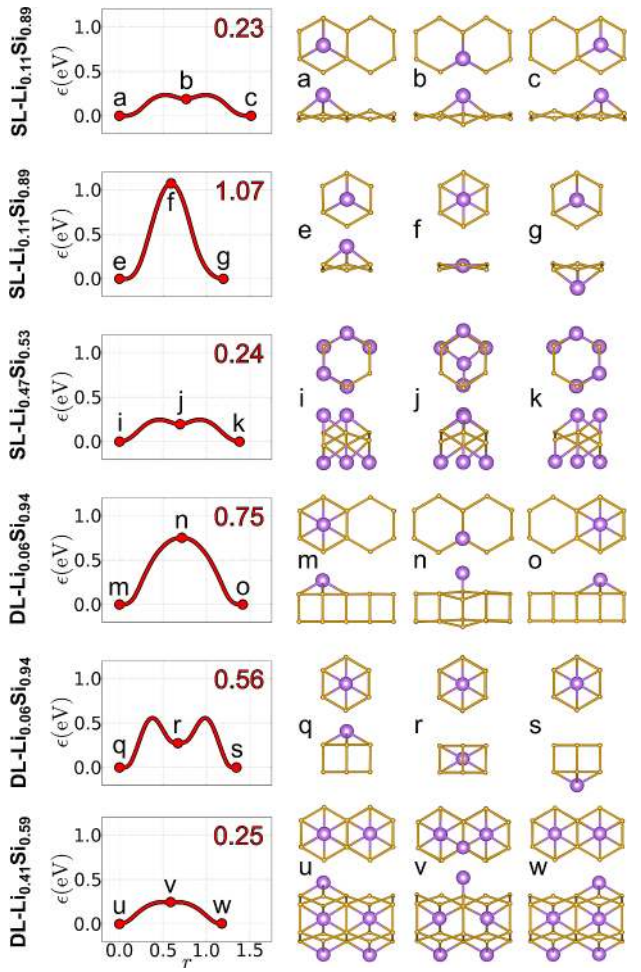

Figure 5. Pathways for the diffusion of atomic Li on single-layer (SL) and double-layer (DL) silicene, Li_xSi_{1-x}, at low (x = 0.11) and high (x > 0.40) Li content. The variation of energy (red solid line) is plotted along the diffusion coordinate r, the latter reported normalized to the lattice constant of each structure (3.88 Å for the single-layer and 4.13 Å for the double-layer). The energy maximum (corresponding to the barrier value) is indicated at the top-right corner of each plot. Initial and final configurations are shown in the left and right columns, respectively, whereas the middle column shows the Li atom (violet) at the middle of the diffusion pathway.

dx.doi.org/10.1021/nl400830u | *Nano Lett.* 2013, 13, 2258−2263

coverage limit, Li resides at the hollow site with three nearest neighbor Si atoms (see also Figure 2). As Li moves between two such adsorption sites, it passes over a Si atom by overcoming an energy barrier of 0.23 eV (Figure 5a–c), which is about three times less than the energy barrier calculated for diffusion in bulk crystalline and amorphous silicon (~0.6 eV).[10,33] At the transition state Li remains bonded to three Si atoms. The total displacement is equal to the lattice constant, a_{sl} = 3.88 Å, while the cumulative sum of the trajectory length of all the atoms in the cell is higher by ~0.5 a_{sl}. Another possibility is Li diffusion from one hollow site to an equivalent one through the silicene layer (Figures 5e-g). This pathway involves an energy barrier of 1.07 eV. In doing so, Li visits the center of the six-atom Si ring where it is surrounded by six nearest neighbor Si atoms. Therefore in-plane diffusion is faster for Li in comparison to diffusion through the silicene layer. An interesting analogy to a thin silicon nanowire can be made where the barrier for Li diffusion on the surface, calculated in previous theoretical work,[34] is significantly lower (<0.2 eV) than that for Li diffusion from the surface to the core region of the nanowire (~0.9 eV). For SL-$Li_{0.47}Si_{0.53}$ (high Li content) Li resides directly above a Si atom (see also Figure 2). In this case, the barrier for Li diffusion is 0.24 eV as Li passes over a hollow site at which point it is bonded to three of the Si atoms in the silicene ring below it.

We discuss next the effect of the additional atomic layer in the double-layer structure of silicene on the energetics of Li diffusion. A single Li adatom hops between two hollow sites on the surface by passing over a Si atom at which point it is bonded to three neighbor Si atoms (Figure 5m–o). The energy barrier along this diffusion pathway is 0.75 eV. We also sampled a diffusion pathway where Li moves through both atomic layers. We find the corresponding energy barrier to be 0.56 eV (Figure 5q–s). Li migrates from one hollow site on one surface to the hollow site on the opposite surface by passing through a closed silicon cage delimited by 12 Si atoms. Therefore, in the low-coverage limit Li diffusion is quite isotropic as in the case of long-range diffusion in bulk amorphous silicon, although double-layer silicene is itself highly anisotropic. On DL-$Li_{0.41}Si_{0.59}$ (high Li content), Li diffuses between two hollow sites by jumping over a Si atom. The corresponding energy barrier is 0.25 eV (Figure 5u–w). There is less distortion in the silicene layer during the diffusion of Li on DL-$Li_{0.41}Si_{0.59}$ in comparison to the case of SL-$Li_{0.47}Si_{0.53}$; compare, for example, the diffusion coordinate between configurations labeled "k" and "w" in Figure 5. To summarize, we find that for both the single-layer and double-layer structures of silicene there exist pathways for Li diffusion with energy barriers that are smaller than or comparable to the energy barriers for diffusion in bulk silicon and thin silicon nanowires.[10,33,34]

From our theoretical findings, we conclude that in contrast to crystalline silicon the silicene layer does not suffer from irreversible structural changes during lithiation and delithiation cycles and the associated change in the effective volume is small (<25%). We identified pathways for Li diffusion with energy barriers smaller than or comparable to those for diffusion in bulk silicon and thin silicon nanowires (<0.6 eV). We found that the number of silicene layers has no significant effect on the energetics of Li adsorption and therefore a different strategy must be employed if increased control over the energetics of Li adsorption is desirable, for example, through doping or the exploration of finite size effects in silicene nanoribbons. The abundance of Si, the high Li capacity of silicene, the flexibility of its atomic layers and the small energy barrier for Li diffusion could prove beneficial for the design of Li-ion batteries based on silicene, which may have high energy density and improved cycle life. Care must be taken for the correct interpretation of our findings, which describe necessary but not sufficient conditions for the design of a high-performance electrode material based on silicene. Further investigation is necessary to determine the conditions under which free-standing silicene can be stable in the environment of a Li-ion battery device during operation. In the work of Lee et al.,[13] a silicon/graphene composite electrode was prepared with high Li-ion storage capacity. With progressively increasing control over the synthesis of two-dimensional structures, we believe that novel materials based on layered silicon for Li-ion storage can indeed become a practical technology.

AUTHOR INFORMATION

Notes

The authors declare no competing financial interest.

ACKNOWLEDGMENTS

Computations were performed on the Odyssey cluster, supported by the FAS Science Division Research Computing Group at Harvard University, the Extreme Science and Engineering Discovery Environment (XSEDE), which is supported by National Science Foundation Grant OCI-1053575, and the SEAS HPC cluster, supported by the Academic Computing Group. S.M. acknowledges financial supports from NSFC (Grant 11222431) and CAS.

REFERENCES

(1) Armand, M.; Tarascon, J.-M. *Nature* **2008**, *451*, 652–657.
(2) Jeong, G.; Kim, Y.-U.; Kim, H.; Kim, Y.-J.; Sohn, H.-J. *Energy Environ. Sci.* **2011**, *4*, 1986–2002.
(3) Kasavajjula, U.; Wang, C.; Appleby, A. J. *J. Power Sources* **2007**, *163*, 1003–1039.
(4) Chan, C. K.; Peng, H.; Liu, G.; McIlwrath, K.; Zhang, X. F.; Huggins, R. A.; Cui, Y. *Nat. Nanotechnol.* **2008**, *3*, 31–35.
(5) Zhao, K.; Tritsaris, G. A.; Pharr, M.; Wang, W. L.; Okeke, O.; Suo, Z.; Vlassak, J. J.; Kaxiras, E. *Nano Lett.* **2012**, *12*, 4397–4403.
(6) Park, M.-H.; Kim, M. G.; Joo, J.; Kim, K.; Kim, J.; Ahn, S.; Cui, Y.; Cho, J. *Nano Lett.* **2009**, *9*, 3844–3847.
(7) Chan, T.-L.; Chelikowsky, J. R. *Nano Lett.* **2010**, *10*, 821–825.
(8) Wu, H.; Chan, G.; Choi, J. W.; Ryu, I.; Yao, Y.; McDowell, M. T.; Lee, S. W.; Jackson, A.; Yang, Y.; Hu, L.; Cui, Y. *Nat. Nanotechnol.* **2012**, *7*, 310–315.
(9) Zhao, K.; Pharr, M.; Cai, S.; Vlassak, J. J.; Suo, Z. *J. Am. Ceram. Soc.* **2011**, *94*, s226–s235.
(10) Tritsaris, G. A.; Zhao, K.; Okeke, O. U.; Kaxiras, E. *J. Phys. Chem. C* **2012**, *116*, 22212–22216.
(11) Castro Neto, A. H.; Guinea, F.; Peres, N. M. R.; Novoselov, K. S.; Geim, A. K. *Rev. Mod. Phys.* **2009**, *81*, 109–162.
(12) Coleman, J. N.; Lotya, M.; O'Neill, A.; Bergin, S. D.; Kingaaa, P. J.; Khan, U.; Young, K.; Gaucher, A.; De, S.; Smith, R. J.; Shvets, I. V.; Arora, S. K.; Stanton, G.; Kim, H.-Y.; Lee, K.; Kim, G. T.; Duesberg, G. S.; Hallam, T.; Boland, J. J.; Wang, J. J.; Donegan, J. F.; Grunlan, J. C.; Moriarty, G.; Shmeliov, A.; Nicholls, R. J.; Perkins, J. M.; Grieveson, E. M.; Theuwissen, K.; McComb, D. W.; Nellist, P. D.; Nicolosi, V. *Science* **2011**, *331*, 568–571.
(13) Lee, J. K.; Smith, K. B.; Hayner, C. M.; Kung, H. H. *Chem. Commun.* **2010**, *46*, 2025–2027.
(14) De Padova, P.; Kubo, O.; Olivieri, B.; Quaresima, C.; Nakayama, T.; Aono, M.; Le Lay, G. *Nano Lett.* **2012**, *12*, 5500–5503.
(15) Meng, L.; Wang, Y.; Zhang, L.; Du, S.; Wu, R.; Li, L.; Zhang, Y.; Li, G.; Zhou, H.; Hofer, W. A.; Gao, H.-J. *Nano Lett.* **2013**, *13* (2), 685–690.

(16) Chen, L.; Liu, C.-C.; Feng, B.; He, X.; Cheng, P.; Ding, Z.; Meng, S.; Yao, Y.; Wu, K. *Phys. Rev. Lett.* **2012**, *109*, 056804.
(17) Feng, B.; Ding, Z.; Meng, S.; Yao, Y.; He, X.; Cheng, P.; Chen, L.; Wu, K. *Nano Lett.* **2012**, *12*, 3507−3511.
(18) Vogt, P.; De Padova, P.; Quaresima, C.; Avila, J.; Frantzeskakis, E.; Asensio, M. C.; Resta, A.; Ealet, B.; Le Lay, G. *Phys. Rev. Lett.* **2012**, *108*, 155501.
(19) Fleurence, A.; Friedlein, R.; Ozaki, T.; Kawai, H.; Wang, Y.; Yamada-Takamura, Y. *Phys. Rev. Lett.* **2012**, *108*, 245501.
(20) Padova, P. D.; Perfetti, P.; Olivieri, B.; Quaresima, C.; Ottaviani, C.; Lay, G. L. *J. Phys.: Condens. Matter* **2012**, *24*, 223001.
(21) Takeda, K.; Shiraishi, K. *Phys. Rev. B* **1994**, *50*, 14916−14922.
(22) Ding, Y.; Ni, J. *Appl. Phys. Lett.* **2009**, *95*, 083115.
(23) Wang, Y.; Scheerschmidt, K.; Gösele, U. *Phys. Rev. B* **2000**, *61*, 12864−12870.
(24) Jose, D.; Datta, A. *Phys. Chem. Chem. Phys.* **2011**, *13*, 7304−7311.
(25) Ruge Quhe, R. F. *Sci. Rep.* **2012**, *2*, 853.
(26) Wang, Y.; Ding, Y. *Solid State Commun.* **2012**, *155*, 6−11.
(27) Cahangirov, S.; Topsakal, M.; Aktürk, E.; Şahin, H.; Ciraci, S. *Phys. Rev. Lett.* **2009**, *102*, 236804.
(28) Houssa, M.; Scalise, E.; Sankaran, K.; Pourtois, G.; Afanas'ev, V. V.; Stesmans, A. *Appl. Phys. Lett.* **2011**, *98*, 223107−223107-3.
(29) Zhang, Q.; Cui, Y.; Wang, E. *J. Phys. Chem. C* **2011**, *115*, 9376−9381.
(30) Cubuk, E. D.; Wang, W. L.; Zhao, K.; Vlassak, J. J.; Suo, Z.; Kaxiras, E. *Nano Lett.* **2013**, DOI: 10.1021/nl400132q.
(31) Osborn, T. H.; Farajian, A. A. *J. Phys. Chem. C* **2012**, *116*, 22916−22920.
(32) Lin, X.; Ni, J. *Phys. Rev. B* **2012**, *86*, 075440.
(33) Wan, W.; Zhang, Q.; Cui, Y.; Wang, E. *J. Phys.: Condens. Matter* **2010**, *22*, 415501.
(34) Zhang, Q.; Zhang, W.; Wan, W.; Cui, Y.; Wang, E. *Nano Lett.* **2010**, *10*, 3243−3249.
(35) Guzmán-Verri, G. G.; Lew Yan Voon, L. C. *Phys. Rev. B* **2007**, *76*, 075131.
(36) Gao, N.; Zheng, W. T.; Jiang, Q. *Phys. Chem. Chem. Phys.* **2011**, *14*, 257−261.
(37) Lebègue, S.; Eriksson, O. *Phys. Rev. B* **2009**, *79*, 115409.
(38) Enkovaara, J.; Rostgaard, C.; Mortensen, J. J.; Chen, J.; Dułak, M.; Ferrighi, L.; Gavnholt, J.; Glinsvad, C.; Haikola, V.; Hansen, H. A.; Kristoffersen, H. H.; Kuisma, M.; Larsen, A. H.; Lehtovaara, L.; Ljungberg, M.; Lopez-Acevedo, O.; Moses, P. G.; Ojanen, J.; Olsen, T.; Petzold, V.; Romero, N. A.; Stausholm-Møller, J.; Strange, M.; Tritsaris, G. A.; Vanin, M.; Walter, M.; Hammer, B.; Häkkinen, H.; Madsen, G. K. H.; Nieminen, R. M.; Nørskov, J. K.; Puska, M.; Rantala, T. T.; Schiøtz, J.; Thygesen, K. S.; Jacobsen, K. W. *J. Phys.: Condens. Matter* **2010**, *22*, 253202.
(39) Blöchl, P. E. *Phys Rev B* **1994**, *50*, 17953.
(40) Perdew, J. P.; Burke, K.; Ernzerhof, M. *Phys. Rev. Lett.* **1996**, *77*, 3865.
(41) Henkelman, G.; Uberuaga, B. P.; Jónsson, H. *J. Chem. Phys.* **2000**, *113*, 9901.
(42) Zhao, K.; Wang, W. L.; Gregoire, J.; Pharr, M.; Suo, Z.; Vlassak, J. J.; Kaxiras, E. *Nano Lett.* **2011**, *11*, 2962−2967.
(43) Sethuraman, V. A.; Chon, M. J.; Shimshak, M.; Srinivasan, V.; Guduru, P. R. *J. Power Sources* **2010**, *195*, 5062−5066.
(44) Tang, W.; Sanville, E.; Henkelman, G. *J. Phys.: Condens. Matter* **2009**, *21*, 084204.